OPEN ACCESS

University of BRISTOL

Lepora, N. F. (2016). Biomimetic Active Touch with Fingertips and Whiskers. *IEEE Transactions on Haptics*, *9*(2), 170-183. [7466131]. https://doi.org/10.1109/TOH.2016.2558180

Publisher's PDF, also known as Version of record

License (if available):
CC BY

Link to published version (if available):
10.1109/TOH.2016.2558180

Link to publication record in Explore Bristol Research
PDF-document

This is the final published version of the article (version of record). It first appeared online via IEEE at http://ieeexplore.ieee.org/xpl/articleDetails.jsp?arnumber=7466131. Please refer to any applicable terms of use of the publisher.

University of Bristol - Explore Bristol Research
General rights

This document is made available in accordance with publisher policies. Please cite only the published version using the reference above. Full terms of use are available:
http://www.bristol.ac.uk/red/research-policy/pure/user-guides/ebr-terms/

Biomimetic Active Touch with Fingertips and Whiskers

Nathan F. Lepora, *Member, IEEE*

Abstract—This study provides a synthetic viewpoint that compares, contrasts, and draws commonalities for biomimetic perception over a range of tactile sensors and tactile stimuli. Biomimetic active perception is formulated from three principles: (i) evidence accumulation based on leading models of perceptual decision making; (ii) action selection with an evidence-based policy, here based on overt focal attention; and (iii) sensory encoding of evidence based on neural coding. Two experiments with each of three biomimetic tactile sensors are considered: the iCub (capacitive) fingertip, the TacTip (optical) tactile sensor, and BIOTACT whiskers. For each sensor, one experiment considers a similar task (perception of shape and location) and the other a different tactile perception task. In all experiments, active perception with a biomimetic action selection policy based on focal attention outperforms passive perception with static or random action selection. The active perception also consistently reaches superresolved accuracy (hyperacuity) finer than the spacing between tactile elements. Biomimetic active touch thus offers a common approach for biomimetic tactile sensors to accurately and robustly characterize and explore non-trivial, uncertain environments analogous to how animals perceive the natural world.

Index Terms—Robotics, tactile devices, perception, touch, active, biomimetic

1 Introduction

Revolutionary progress over the last two decades in neuroscience/psychology and robotics has enabled these fields to directly inform each other: life can be mimicked *vita in machina*. This synthesis between the living and the artificial is captured by the research field of biomimetics, which is the development of novel technologies through the distillation of principles from the study of biological systems. In consequence, there has recently been an explosion of new discoveries in biomimetics [1].

Here we study the biomimetics of perception in the modality of touch. A principal aspect of tactile perception, and arguably all natural perception, is that touch is actively controlled: we do not just touch, we feel [2], [3]. Consequently, tactile sensation, perception and action should not be considered simply as a forward process, but instead a closed 'active perception' loop.

There are two aspects of biomimetics in the present study. First, we use three distinct tactile sensors that are designed and constructed around biomimetic principles. Two are biomimetic fingertips: the iCub (capacitive) fingertip [4] and the TacTip [5], an optical tactile sensor. Sensing elements within these fingertips mimic mechanoreception in human touch, with both sensors having a discrete 'taxel' structure embedded in a compliant skin, giving broad overlapping receptive fields necessary for perceptual hyperacuity (superresolution) [6], [7]. The third sensor uses biomimetic BIOTACT whiskers that mimic rodent vibrissae in both their morphology and sensing (mechanoreception) capabilities [8], [9].

The second aspect of biomimetics in this study is that the algorithms for perception are based on principles underlying biological perception. Biomimetic perception is here formulated from three principles: first, decision making based on evidence accumulation models from perceptual neuroscience; second, action selection during the decision process; and third, neuronal sensory encoding to generate evidence for perception. The perception is active if the action selection uses evidence gathered from the decision process [2], and passive for random or static actions independent of sensory evidence. Here we consider biomimetic active perception based on human and animal focal attention [10], where evidence for stimulus location is used to move the sensor onto the object.

The main contribution of this study is to provide, for the first time, a synthetic viewpoint that compares, contrasts and draws commonalities for active perception deployed over a range of biomimetic tactile sensors and stimuli. We thus consider two distinct experiments for each sensor (TacTip, iCub fingertip and BIOTACT whiskers), with the first experiment essentially the same to permit direct comparison across sensors (taps against cylinders with varying contact location), while the second experiments cover a broad range of different tactile features to demonstrate the generality of the approach (gap width with depth, textured surfaces with depth, and contact speed with radial distance).

We conclude that although these three tactile sensors appear *prima facie* rather different from each other, they share an underlying commonality that enables them to benefit from a common approach to biomimetic active perception. This commonality stems from sharing a biomimetic design comprised of discrete sensing elements with overlapping receptive fields, and being utilized in situations of uncertain stimulus location ('where') and identity ('what') akin to the

• *The author is with the Department of Engineering Mathematics, and Bristol Robotics Laboratory, The University of Bristol, Bristol, United Kingdom. E-mail: n.lepora@bristol.ac.uk.*

Manuscript received 14 June 2015; revised 16 Mar. 2016; accepted 20 Mar. 2016. Date of publication 6 May 2016; date of current version 15 June 2016. Recommended for acceptance by M. Santello.
For information on obtaining reprints of this article, please send e-mail to: reprints@ieee.org, and reference the Digital Object Identifier below.
Digital Object Identifier no. 10.1109/TOH.2016.2558180

This work is licensed under a Creative Commons Attribution 3.0 License. For more information, see http://creativecommons.org/licenses/by/3.0/

uncertain environments animals also face. In consequence, we propose that biomimetic active touch offers a common approach for tactile robots to accurately and robustly characterize and explore non-trivial, uncertain environments analogous to how animals perceive the natural world.

2 Background and Related Work

Concepts related to active tactile perception and active touch have been defined by several scientists over the last 50 years [11], [12]. In his 1962 article on "Observations on Active Touch", psychologist J.J. Gibson observes that: "The act of touching or feeling is a search for stimulation... the movements of the fingers are purposive. An organ of the body is being adjusted for the registering of information" [13]. In her 1988 paper on "Active Perception", engineering scientist R. Bajcsy used the term active to denote "purposefully changing the sensor's state parameters according to sensing strategies," such that these controlling strategies are "applied to the data acquisition process which will depend on the current state of the data interpretation and the goal or the task of the process" [2]. As such, her definition of active perception is a rephrasing of Gibson's description of active touch using a terminology appropriate to engineering artificial systems [12].

Closely related to active touch perception, the concept of 'Haptic Exploration' was introduced in psychologists S. Lederman and R. Klatzky's 1987 article on "Hand Movements: A Window into Haptic Stimulus Recognition" [14]. They propose that "the hand (more accurately, the hand and brain) is an intelligent device, in that it uses motor capabilities to greatly extend its sensory functions," consistent with observations on active touch by Gibson and others. Like Gibson, they emphasize the purposive nature of the movements guiding the hand and fingers to recognize stimuli, but they go further in proposing the motor mechanisms (exploratory procedures) that constitute those purposive movements.

Around the time of the above work on active perception [2] and haptic exploration [14], there were several initial proposals basing robot touch on related principles [15], [16]. Early examples of active perception with tactile fingertips came soon after, including controlling a tactile fingertip for profile delineation of an unseen stimulus [17] and to measure surface roughness [18]. Implementations of haptic exploration with dexterous robot hands followed, both with exploratory procedures where some fingers grasp and manipulate while others feel the stimulus surface [19] and using active perception to guide grasping [20]. A survey of early work in these areas can be found in [21].

Recent work on active perception with biomimetic fingertips has focussed on algorithms for sensor control and perception. An artificial finger that can dynamically feel texture [22] used a neural network controller for curiosity-driven exploration to learn motor skills for active perception [23]. Another study used closed loop control of exploratory movements with a biomimetic fingertip to discriminate the compliance of materials [24].

There has also been interest in probabilistic approaches for active perception. An implementation of 'Bayesian exploration' selected movements that best disambiguate a percept, and was applied to a large database of textures with control of contact force and speed [25], [26]. Another study classified data from multiple exploratory procedures to learn haptic adjectives [27]. A theoretical framework used Bayesian models of perception and exploration as a tactile attention mechanism [28]. Closely related to the present study, an implementation of 'active Bayesian perception' selected movements based on intermediate estimates of the percepts to fixate on a good region for perception [10], [29], [30]. This approach can improve the quality of the perception to attain robust tactile superresolution sensing [6], [7], applies to tactile manipulation [31], [32] and extends to exploratory procedures such as contour following [33].

Active perception has also been demonstrated on whiskered robots. Early work included using an 'active antenna' to detect contact distance [34] and an 'active artificial whisker array' for texture discrimination [35]. These early studies used 'active' to mean the sensor is moving, but did not consider a feedback loop to modulate the whisking. Later whiskered robots implemented sensorimotor feedback between the tactile sensing and motor control [36], [37] enabling demonstration of the contact dependency of texture perception with a whiskered robot [38] and that texture perception was improved when the whisking motion was controlled using a sensory feedback mechanism [8].

3 Biomimetic Tactile Sensors

3.1 Optical Tactile Fingertip (TacTip)

The TacTip (*Tac*tile finger*Tip*) is a biomimetic tactile sensor developed at Bristol Robotics Laboratory [5], [7], [30], [31], [32], [39], [40] that was designed to mimic aspects of human tactile sensing. The TacTip's principal novelty as an optical tactile sensor is that it has a fine array of pins molded on the inside of the skin that indicate deformations of the sensor surface. These pins are analogous to the tactile sensing structure of the human fingertip: the *dermal papillae*, which are small pimple-like extensions of the dermis (inner fatty layer of skin) into the epidermis (outer skin layer). In the human skin, these papillae are highly innervated with tactile mechanoreceptors to detect vibration and light touch. In the biomimetic TacTip, the papillae enable measurement of deformations of the sensor surface as their positions are tracked with an internally mounted CCD camera.

From an engineering point of view, the TacTip has several highly useful properties: (i) the casing is 3D-printed and hence readily customizable and inexpensive; (ii) it uses a standard CCD web-camera (LifeCam Cinema HD, Microsoft) to collect data, which is also inexpensive and connects to a PC via a USB interface; (iii) it has a molded silicone outer membrane that is robust to wear and easily replaced if damaged; and (iv) between the outer membrane and the electronics is a clear compliant gel (RTV27906, Techsil UK) that both enables tactile sensing through compression and protects the delicate parts of the sensor.

The particular design of TacTip used here has a 40 mm diameter hemispherical sensor pad with 532 pins arranged in a regular array on its underside. Six LEDs are mounted on a ring around the base of the pad to illuminate the pins, whose tips are white to contrast with the black silicone outer membrane. Pins were tracked using optical flow by applying the Lucas-Kanade algorithm to a monochrome stack of images [7] (resolution 640×480 pixels, sampling rate 20 fps). From these, a subset of pins were selected to reduce computational load

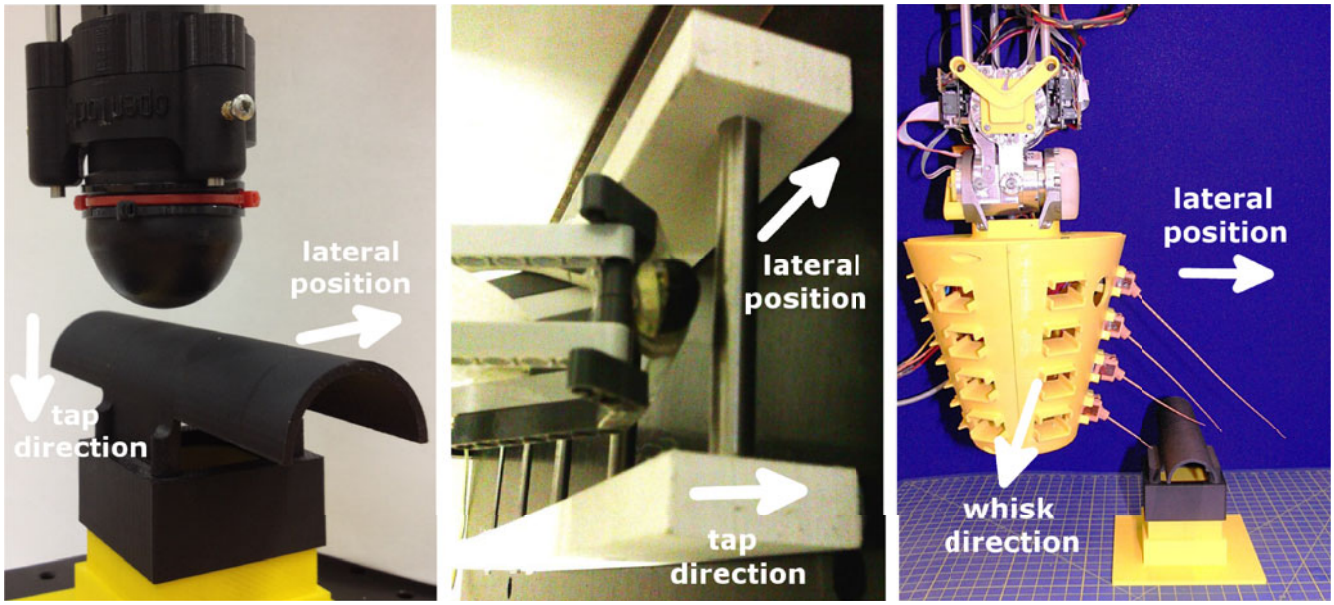

(a) Optical tactile fingertip (the TacTip) mounted on an ABB 6-dof robot arm

(b) Capacitive tactile fingertip (iCub fingertip) mounted on a Yamaha 2-dof Cartesian robot

(c) Tactile whisker array (G1 sensor) mounted on an Elumotion 7-dof robot arm

Fig. 1. Biomimetic tactile sensors mounted as end-effectors to robot arms (a,c) and on a Cartesian robot (b) considered in this study.

and redundancy (36 pins; 4 mm separation) to give $N_{\text{dims}} = 72$ sensor dimensions.

Here the TacTip (Fig. 1a) is mounted as an end effector on a six degree-of-freedom robot arm (IRB 120, ABB Robotics). The arm can precisely and repeatedly position the sensor (absolute repeatability 0.01 mm), making it ideal for probing tactile sensing.

3.2 Capacitive Tactile Fingertip (iCub Fingertip)

Capacitive sensor technology is popular in robotics because it has the promise to be cheaply fabricated in small sizes over curved surfaces, permitting its construction and integration into dense arrays across areas such as biomimetic fingertips and palms [4], [41]. Other advantages include high sensitivity, long-term drift stability, low temperature sensitivity and low power consumption [42].

The iCub fingertip is a biomimetic tactile sensor constructed for the iCub humanoid robot [4], a child-sized robot developed at the Italian Institute of Technology (IIT) that has an anthropomorphic body design and sensor capabilities [43]. The iCub fingertip has a rounded shape that resembles a human fingertip and a compliant outer surface that enables pressure sensing via compression. Pressure sensing is via discrete overlapping taxels (tactile elements), mimicking aspects of mechanoreception in human touch [44], [45]; for example, the taxel receptive fields are broader than the taxel spacing with a sensitivity that peaks in the center and decreases gradually away from that peak [6].

The particular design of the iCub fingertip used here has a rounded shape 14.5 mm long by 13 mm wide and 13 mm deep. A hard inner support is wrapped with a flexible printed circuit board (PCB) with conductive patches for the touch sensor 'taxels' spaced 4.5 mm apart. The PCB is covered first with a $\sim$2 mm layer of non-conductive soft silicone foam and then with a thin layer of conductive silicone rubber maintained at an isopotential. Pressure (capacitance) readings are sampled at 50 Hz with 8-bit encoding for each for each of the $N_{\text{dims}} = 12$ taxels.

Here the iCub tactile fingertip (Fig. 1b) is mounted as an end effector on a two degree-of-freedom Cartesian robot (2-axis PXYx, Yamaha Robotics). This combination of tactile sensor with Cartesian robot has been employed previously for testing various sensors, including tactile vibrissae [46], [47] and tactile fingertips [10], [29], [48], [49]. The Cartesian robot is able to precisely and repeatedly position the sensor in two dimensions (absolute repeatability 0.02 mm) with simple control, making it a good platform to probe tactile sensing in basic one-dimensional scenarios with contacts controlled in the other dimension.

3.3 Tactile Whiskers (BIOTACT Vibrissae)

Vibrissal sensing is of interest to engineers because artificial vibrissae provide proximal sensors that can determine distance to nearby stimuli alongside surface characteristics such as shape and texture [37], [50]. Vibrissal sensors could be employed in circumstances where vision is compromised but there is a need for light contact, such as hazardous environments containing smoke or dust, or in darkness where there is a need to operate covertly.

The BIOTACT vibrissae are a component of a novel biomimetic tactile sensing system based on the facial whiskers of rodents such as rats and mice [8], [9] that was developed at Bristol Robotics Laboratory and the University of Sheffield for the EU FP7 project *BIOmimetic Technology for vibrissal ACTive touch*. The whiskers are instrumented at the base to detect deflections of the shaft by surface contact, analogous to how mechanoreceptors at the base of biological whiskers respond to encode information about the nature of a contact. Their vibrissal morphology is also biomimetic including the physical characteristics (tapered shafts, bending and relative lengths) of individual whiskers.

Two systems for mounting and controlling the whiskers were considered. The first mounted the whiskers in a

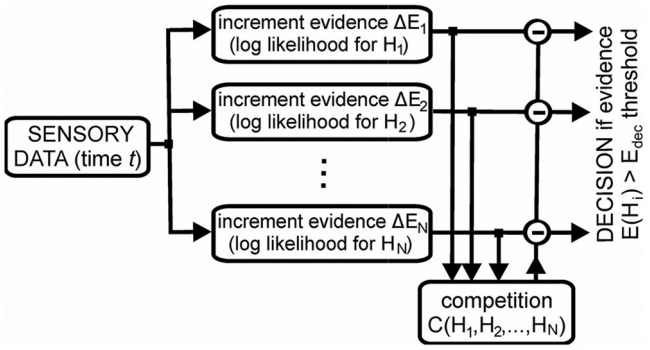

Fig. 2. Decision making process. Evidence is accumulated for multiple distinct perceptual hypotheses, to choose the percept with maximal accumulated evidence when the evidence crosses a threshold.

truncated conical head (Fig. 1c) holding up to 24 whisker modules arranged in six radially symmetric rows of four [8]. For the present experiments only one row of four whiskers was populated, appropriate to localization along a single dimension. Whiskers towards the front were shorter than at the back (lengths 50, 80, 115 and 160 mm), with tips ~30 mm apart when forward extended. The head is mounted as the end-effector of a 7-degree-of-freedom robot arm (El-arm, Elumotion) that can move and orient the BIOTACT system in its work space (absolute repeatability 0.1 mm).

A second whisker system was deployed with a single non-actuated whisker (length 160 mm) mounted on the two degree-of-freedom Cartesian robot described above (Section 3.2), to enable accurate testing of single whisker sensing capabilities. For both systems, the 2D deflections upon contacting stimuli were measured with a hall effect sensor at the base of each whisker, giving $N_{\rm dims} = 8$ and 2 sensor dimensions on the two systems, respectively. All data were sampled at 1 kHz with processing/control executed under the BRAHMS Modular Execution Framework [51].

4 Biomimetic Tactile Perception

Here we formulate biomimetic tactile perception from three principles based on biological perception (Fig. 4): (i) an underlying *decision making* part based on leading models from perceptual neuroscience; (ii) an *action selection* part enacted during the decision making, which includes active movement strategies based on human and animal focal attention; and (iii) *sensory encoding* of how percepts relate to stimuli, here considered as a probabilistic model having analogues with neural coding.

4.1 Decision Making

The first component of biomimetic tactile perception is to implement decision making in an artificial system. A diverse range of studies of biological systems indicate three shared computational principles underlying natural decision formation (*c.f.* [52], [53], [54]). The first common principle is that sensory information is represented as evidence for the decision alternatives; for example, the rate of protein binding in a signalling pathway of a bacterium, the neuronal activity in the brain of an animal, and the population densities of bees returning from potential nest sites in a swarm. The second principle is that evidence accumulates until reaching a threshold that triggers a decision; this includes, the concentration to switch a gene in a cell, the activation level for a motor neuron, or the quorum number to reach swarm consensus. The last common principle is competition between alternatives, in that evidence for one outcome disfavors all others; examples include competition for protein binding between cells, inhibition between neurons in the brain, and recruitment of bees from one potential nest site to another in a swarm.

Remarkably, these three computational principles also underlie the statistical technique of Bayesian sequential analysis for making optimal decisions under uncertainty. Sequential analysis is a statistical technique for hypothesis selection over data that is sequentially sampled until reaching a stopping condition [55], which commonly takes the form of a threshold on the posterior belief. Because this evidence is derived from probability distributions, there is necessarily a competition between alternatives, since the probabilities for all options must sum to one (and so evidence for one alternative disfavors all others). Consequently, sequential analysis has been applied widely to modeling decision formation in biological systems, including single cellular organisms (e.g., [52]), perceptual decision making in animals and humans (e.g., [53]) and collective animal behavior (e.g., [54]).

To emphasize the relation with biological decision making, here we re-express sequential analysis explicitly in terms of evidence accumulation to threshold with competition (Fig. 2) [56]. We consider situations in which a sensor makes successive contacts z_t ($t = 1, 2, \ldots$) with a stimulus of interest, such that each contact gives an increment of evidence ΔE_t for the alternatives

$$E_t(H_h) = \Delta E_t(H_h) + E_{t-1}(H_h) - C_t(H_1, \ldots, H_N) \quad (1)$$

over $1 \leq h \leq N$ distinct perceptual hypotheses $H_1, \ldots, H_N$. Competition between the alternative hypotheses is represented by a term $C_t(H_1, \ldots, H_N)$ that is a function of the evidence $E_t(H_1), \ldots, E_t(H_N)$ for all alternatives. Decision termination occurs at a threshold level of accumulated evidence

$$\text{if any} \quad E_t(H_h) \geq E_{\rm dec} \quad \text{then} \quad H_{\rm dec} = \arg\max_{H_h} E_t(H_h) \quad (2)$$

when the perceptual hypothesis with the most evidence is taken as the decided alternative.

The above evidence update relates to Bayesian inference if the increment of evidence is defined as the log likelihood of the contact data z_t over the perceptual hypotheses

$$\Delta E_t(H_h) = \log P(z_t|H_h). \quad (3)$$

Then the evidence update rule is equivalent to recursive Bayesian inference over all independent contacts $z_{1:t}$, with the accumulated evidence the log posterior belief

$$E_t(H_h) = \log P(H_h|z_{1:t}) \quad (4)$$

provided the competition term is the log marginal (normalizing) term in Bayes' rule

$$C_t = \log P(z_t|z_{1:t-1}) = \log \sum_{h=1}^{N} P(z_t|H_h)P(H_h|z_{1:t-1}). \quad (5)$$

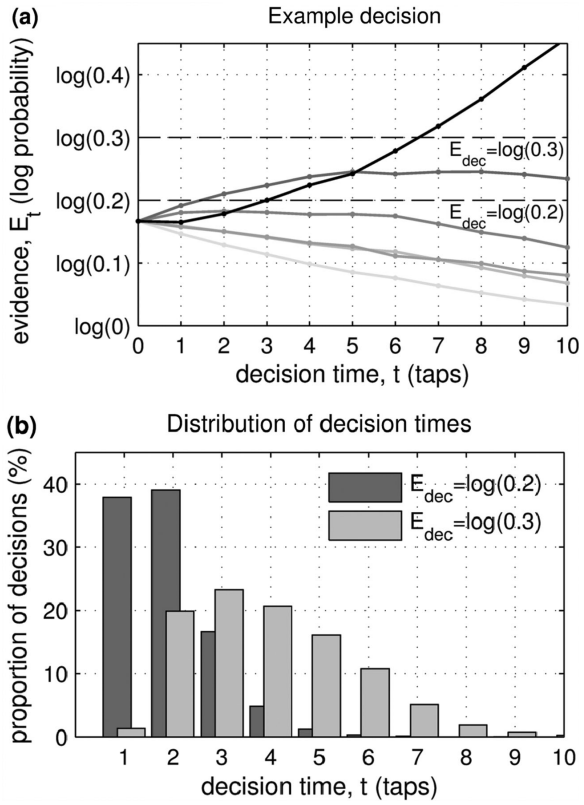

Fig. 3. (a) Example dependence of decision on threshold: quicker but more inaccurate decisions are made for a lower threshold (results compared for $E_{\mathrm{dec}} = \log(0.2)$ versus $\log(0.3)$; correct response in black). (b) Decision time histograms for these thresholds over many examples.

Note that with these definitions, the evidence has a negative range; however, if positive values are desired, the entire range can be renormalized with an additive constant [57]. The equivalence with Bayes' rule is shown by substituting equations (3-5) into the evidence update (1) and combining logarithms.

Accordingly, the evidence update to threshold can be interpreted as multi-alternative Bayesian sequential analysis, since the evidence threshold is equivalent to a threshold on the posterior belief and a *maximum a posteriori* decision rule

$$\text{if any} \quad P(H_h|z_{1:t}) \geq \theta_{\mathrm{dec}} \text{ then } H_{\mathrm{dec}} = \arg\max_{H_h} P(H_h|z_{1:t}) \tag{6}$$

with threshold given by $E_{\mathrm{dec}} = \log\theta_{\mathrm{dec}}$. This decision threshold θ_{dec} is a free parameter that adjusts the balance between decision time t_{dec} and accuracy e_{dec}. Given the evidence is sampled stochastically, there is a distribution of decision times and decision outcomes that depends on the decision threshold (Fig. 3). For choices between two outcomes the speed-accuracy balance can be proved optimal [55]; optimality is not known for the many perceptual choices considered here, so we make a reasonable assumption of near optimality [56].

4.2 Action Selection

The second component of biomimetic active perception is the selection between alternative actions during perception (i.e., deciding 'where to move next'). Action selection is a general problem facing all autonomous agents, both biological and artificial, and thus research in action selection spans ethology, psychology, neurobiology, computational neuroscience, artificial intelligence and robotics [58], [59]. Action selection is related to attention, because overt shifts of attention are also selected actions; in contrast, covert shifts of attention (with no explicit movement) appear more closely related to internal selection of processing resources. Here we implement biomimetic active touch as an overt attention mechanism (Fig. 4), although later extensions of the formalism could also include covert attention if necessary.

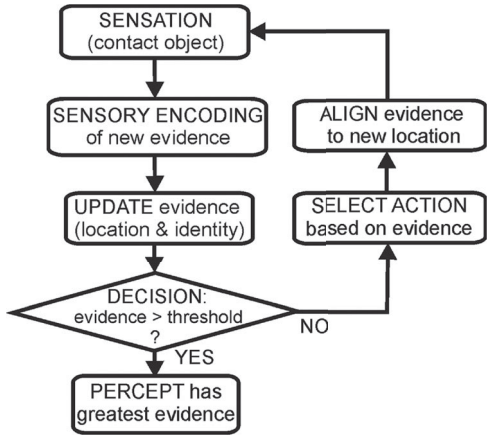

Fig. 4. Biomimetic active perception is implemented as a sensation-action loop in which evidence is accumulated for multiple distinct perceptual hypotheses. During the decision process, a control policy selects appropriate actions to relocate the sensor based on the accumulated evidence. The decision is made when the accumulated evidence passes a decision threshold, choosing the percept with maximal evidence.

Formally, action selection can be defined as follows [58]: given an agent with a choice of possible actions, a stored internal state, and externally-derived sensory information, the task is to decide which action the agent should perform to best attain its goals. Here the goal of the action selection is to optimize tactile perception according to the speed and accuracy of the decision making component of the biomimetic tactile perception (Section 4.1). Accordingly, the internal state will be be accumulated evidence $E_t(H_h)$ for the alternatives and the sensory information will be encoded within that evidence as each increment ΔE_t.

To formulate our action selection mechanism, we suppose that the N perceptual hypotheses H_h are a product of N_{loc} location 'where' x_l and N_{id} identity 'what' w_i classes, with evidence

$$E_t(H_h) = E_t(x_l, w_i), \tag{7}$$

distributed over $N = N_{\mathrm{loc}}N_{\mathrm{id}}$ 'where-what' percepts, in which $h = (l, i)$ represents $h = (l-1)N_{\mathrm{id}} + i$. For example, the stimulus being perceived could be one of N_{id} types (e.g., cylinders of distinct diameters) with its location perceived as one of N_{loc} distinct positions. Here we take the location x_l percepts as pertaining to degrees of freedom that can be actively controlled (e.g., contact position); conversely, the identity percepts w_i are those dimensions beyond the agent's control, such as those intrinsic to the stimulus being identified (e.g., stimulus curvature or texture) [10].

Action selection can then be included as an attentional mechanism within the decision making process by defining a movement policy that shifts the (unknown) location x by

an amount Δx, enacted after each increment of evidence ΔE_t

$$\begin{aligned} &\Delta x = \pi(E_t(x_l, w_i)), \\ &x \leftarrow x + \Delta x. \end{aligned} \tag{8}$$

(The left arrow denotes that the quantity on the left is replaced with that on the right.) This policy will depend on the present evidence $E_t(x_l, w_i)$ over all location and identity classes, but not on the present location x which is assumed unknown. In practise, the policy will be defined here as a discrete shift in the location class index, such that $x_l \leftarrow x_l + \Delta x = x_{l+\Delta l}$; for example, with position classes spaced every 1 mm, the policy gives integer movements $\Delta x = \Delta l$ mm.

Here we define the location 'where' classes x_l of the stimulus relative to the sensor (an *egocentric* frame of reference), so that the increments of evidence $\Delta E_t(x_l, w_i)$ stay at the same relative locations x_l with respect to the sensor. However, if the stimulus is fixed relative to the world (in an *allocentric* frame), an action will change the location of sensed evidence relative to the sensor. To correct for this mismatch between allocentric and egocentric coordinates, after each action a compensatory shift in the location component of the evidence is implemented

$$\begin{aligned} &E_t(x_l, w_i) \leftarrow E_t(x_{l-\Delta l}, w_i) \text{ if } 1 \le x_{l-\Delta l} \le N_{\text{loc}} \\ &\text{else } E_t(x_l, w_i) \leftarrow E_t(x_1, w_i) \text{ or } E_t(x_{N_{\text{loc}}}, w_i). \end{aligned} \tag{9}$$

For simplicity, the (undetermined) evidence shifted from outside the location range is assumed uniform and given by the existing evidence at that extremity of the range.

The evidence-based decision making and action selection components of our algorithm for biomimetic active touch are shown in Fig. 4. For this study, we consider three distinct action selection policies to illustrate biomimetic touch (described below and illustrated in Fig. 5).

4.2.1 Action Selection Policy 1: Active Focal Attention

The first action selection policy is inspired by human and animal focal attention, where the fovea of the eye is actively fixated to center on a stimulus during perception. This is implemented here with an attempted move to a fixation point x_{fix} on the stimulus

$$\Delta x = \pi(E_t) = x_{\text{fix}} - x_{\text{est}}(E_t) \tag{10}$$

using the currently estimated location at the peak evidence

$$x_{\text{est}} = \arg\max_{x_l} \sum_{i=1}^{N_{\text{id}}} E_t(x_l, w_i). \tag{11}$$

If the estimate of contact location is accurate $x_{\text{est}} = x$, then this policy will converge on the fixation point, as shown by the example trajectories in Fig. 5a. The policy is active because the action selection depends on the accumulated evidence.

The fixation point x_{fix} is a free parameter that specifies the active control strategy to attain focal attention, and remains fixed throughout an episode of tactile decision making. In practise, we determined the fixation point for the six experiments on a case-by-case basis, using an assessment of how the perception depends on the location where the stimulus is sensed (Section 6).

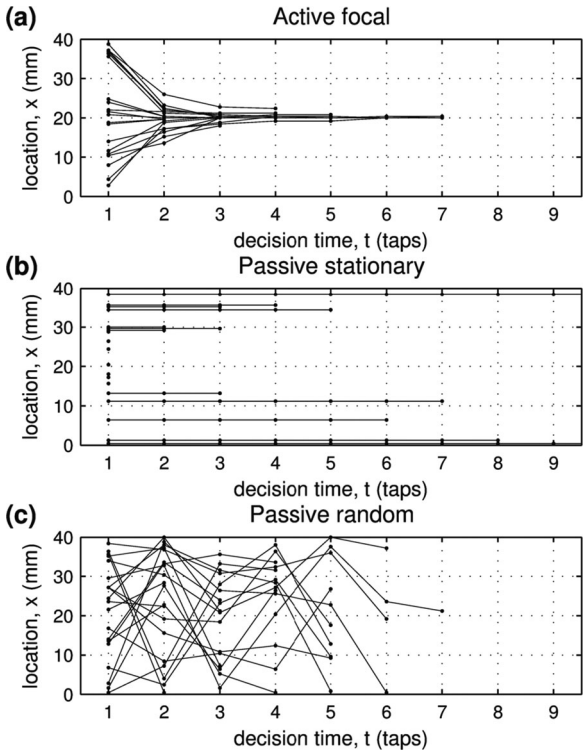

Fig. 5. Example trajectories for active and passive tactile perception. In each case, 20 trajectories with random initial condition were generated from the TacTip perceiving cylinders (Fig. 6a), as analyzed in Figs. 7a and 8a.

4.2.2 Action Selection Policy 2: Passive Stationary

We contrast the above (active) action selection with a policy for stationary passive perception, where the sensor does not move outside the location class that it initially contacts the stimulus:

$$\Delta x = \pi(E_t) = 0. \tag{12}$$

This policy is known as passive because it does not depend on the accumulated evidence E_t. Example trajectories for this policy are shown in Fig. 5b, which as expected are constant in time. Note there are no free parameters in this policy.

4.2.3 Action Selection Policy 3: Passive Random

Another action selection policy for passive perception randomly chooses each contact location x_l within its range before sampling the next increment of evidence:

$$\Delta x = \pi(E_t) \sim U(1, x_{N_{\text{loc}}}) \tag{13}$$

from a uniform distribution $\Delta x \sim U(1, x_{N_{\text{loc}}})$, $p(x) = 1/N_{\text{loc}}$. For the move to give a contact location in range, the resulting locations $1 \le x + \Delta x \le N_{\text{loc}}$ are defined modulo N_{loc}. This policy is passive because it does not depend on the accumulated evidence E_t. Example trajectories are shown in Fig. 5c; note again there are no free parameters in this policy.

4.3 Sensory Encoding

The third component of biomimetic active perception is to encode the sensory data as evidence that can be used for the decision making in Section 4.1 and attentional action

TABLE 1
Details of the Six Experiments Considered in This Study (Two for Each of the TacTip, iCub Fingertip, and BIOTACT Whiskers)

Sensor	Location (number: range)	Identity (number: range)	Classes: N_{loc} (range), N_{id} (range)	Contact data ($N_{\text{samps}}, N_{\text{dims}}$)
TacTip	Lateral position (1000: 0-40 mm)	Cylinders (6: 30-80 mm dia.)	100 (0.4 mm), 6 (10 mm)	2 sec tap (30 samples, 36×2 taxel dims)
	Contact depth (110: 0-5 mm)	Gap width (20: 0.25-5 mm)	11 (0.5 mm), 20 (0.25 mm)	2 sec tap (30 samples, 36×2 taxel dims)
iCub fingertip	Lateral position (3000: 0-30 mm)	Cylinders (5: 4-12 mm dia.)	100 (0.3 mm), 5 (2 mm)	1 sec tap (50 samples, 12 taxels)
	Contact depth (150: 0-3 mm)	Texture (12: p60-p800)	15 (0.2 mm), 12 (1 grade)	1 sec tap (50 samples, 12 taxels)
BIOTACT whisker	Lateral position (400: 0-100 mm)	Cylinders (6: 30-80 mm dia.)	40 (2.5 mm), 6 (10 mm)	1 sec whisk (1000 samples, 4×2 dims)
	Radial distance (100: 30-80 mm)	Speed (100: 72-210 mm/sec)	10 (10 mm), 20 (9 mm/sec)	1.5 sec whisk (1500 samples, 4×2 dims)

selection in Section 4.2. The encoding of data as evidence is learned from training data that is distinct from the testing data used to assess performance.

To further emphasize the relation with biological decision making, we model the increment of evidence ΔE for each percept H_h in a form resembling neuronal spatial and temporal summation

$$\Delta E(H_h) = \frac{1}{N^{\text{test}}_{\text{samps}}} \sum_{d=1}^{N_{\text{dims}}} \sum_{f=1}^{N_{\text{features}}} \sum_{j=1}^{N^{\text{test}}_{\text{samps}}} w_{df}(H_h)\, n_{df}(j). \quad (14)$$

The synaptic weights w_{df} depend on the percept H_h and are learnt from training data. The spike events n_{df} depend on the test sample time j and are the result of passing the sensory test data through a collection of binary-valued (0 or 1) feature detectors

$$n_{df}(j) = F_f(s_d(j)), \quad 1 \le f \le N_{\text{features}}. \quad (15)$$

The sensory data $s_d(j)$ has spatial dimension d labeling the receiving receptor (here a pin dimension, taxel or whisker) and temporal dimension j labeling the test sample within a contact,

$$z = \{s_d(j) \ : \ 1 \le j \le N^{\text{test}}_{\text{samps}},\ 1 \le d \le N_{\text{dims}}\}. \quad (16)$$

Thus, sensory evidence derives from transducing a sensory contact (tap or whisk) into a spatial array of temporally distributed events across tactile features and receptors, which are weighted, summed, then normalized over the duration of the contact.

The above model of sensory evidence relates to Bayesian inference via the expression (3) for evidence as a log likelihood

$$\Delta E(H_h) = \log P(z|H_h) = \sum_{d=1}^{N_{\text{dims}}} \sum_{j=1}^{N^{\text{test}}_{\text{samps}}} \frac{\log P_d(s_d(j)|H_h)}{N^{\text{test}}_{\text{samps}} N_{\text{dims}}} \quad (17)$$

and modeling all data dimensions d and test samples j as independent (so the single log likelihoods for each sample sum). This likelihood model is normalized by the total number of data points $N^{\text{test}}_{\text{samps}} N_{\text{dims}}$ to ensure that evidence does not scale with the number of samples in a contact (so varying sample numbers between contacts gives similarly scaled evidence), which can also be justified from the combinatorics of the probabilities [60]. The independence assumption, while violated in practice, is standard in statistics and makes the likelihood calculation tractable.

The evidence model (17) is then defined by likelihood models $P_d(s_d|H_h)$ for each data dimension d (pin, taxel or whisker) and each perceptual hypothesis H_h (location x_l and identity w_i class). For likelihood models constructed from histograms, which have been standard in past work on tactile perception [56], [61], we can then obtain the form of evidence (14) analogous to neuronal spatiotemporal summation, as we now show.

For likelihood models based on histograms, the feature detectors (15) measure the occupancy of samples binned into equal intervals I_f, $1 \le f \le N_{\text{bins}}$, spanning the training data range

$$n_{df} = F_f(s_d) = \begin{cases} 1, & s_d \text{ in interval } I_f \\ 0, & \text{otherwise.} \end{cases} \quad (18)$$

(Here we typically use $N_{\text{features}} = N_{\text{bins}} = 100$ equal bins.) Given training data $z(H_h)$ with $N^{\text{train}}_{\text{samps}}$ samples $s_d(j)$ as in (16) for percept H_h, the log likelihoods are then

$$\log P_d(s_d|H_h) = \log \frac{\sum_{j=1}^{N^{\text{train}}_{\text{samps}}} n_{df}(j)}{\sum_{f=1}^{N_{\text{bins}}} \sum_{j=1}^{N^{\text{train}}_{\text{samps}}} n_{df}(j)} \text{ for } s_d \text{ in } I_f. \quad (19)$$

Technically, these log likelihoods are ill-defined if any histogram bin count n_{df} is empty, which is fixed by regularizing (replacing) the zero in (18) with a small constant ($\epsilon \ll 1$).

Therefore if the trained weights for each percept are

$$w_{df}(H_h) = \frac{1}{N_{\text{dims}}} \log P_d(s_d|H_h) \text{ for } s_d \text{ in } I_f \quad (20)$$

then (upon substituting (20) into (14) to obtain (17)) the evidence expressed as a log likelihood is equivalent to the form resembling neuronal spatial and temporal summation, as claimed at the beginning of this section.

5 Experimental Validation Methodology

5.1 Experimental Datasets

Here we consider two distinct types of experiment for each of the three tactile sensors (TacTip, iCub fingertip and BIOTACT whiskers); the resulting six data sets are summarized in Table 1, with one set for each sensor shown in Fig. 6. All sets consist of collections of contact data taken over various locations and stimulus identities. Each contact is a discrete tap (fingertip) or whisk (whisker) onto then off the stimulus of interest. For simplicity and consistency across the sets, only one dimension for location and one for identity are

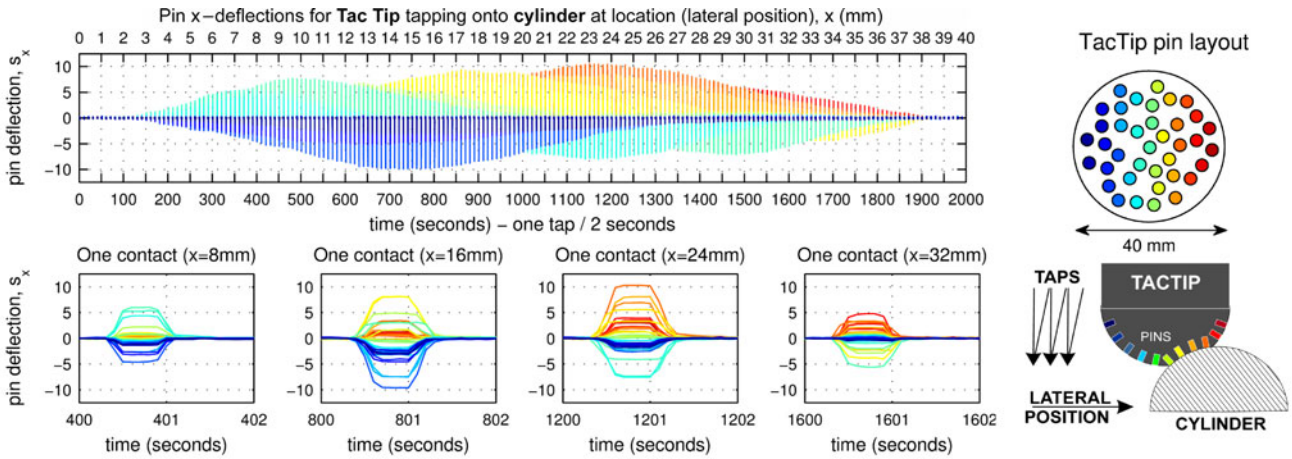

(a) Data for the optical tactile fingertip (the TacTip) tapping onto a cylinder (50 mm dia.) at location x (lateral position). Top: entire data set of 4000 taps over 40 mm range, plotted against time (each tap takes 2 secs). Bottom 4 panels: contact data from individual taps. The color of the plotted trace corresponds to the pin locations (right figure) and its magnitude the pin x-deflection (a similar plot can be made for the y-deflections).

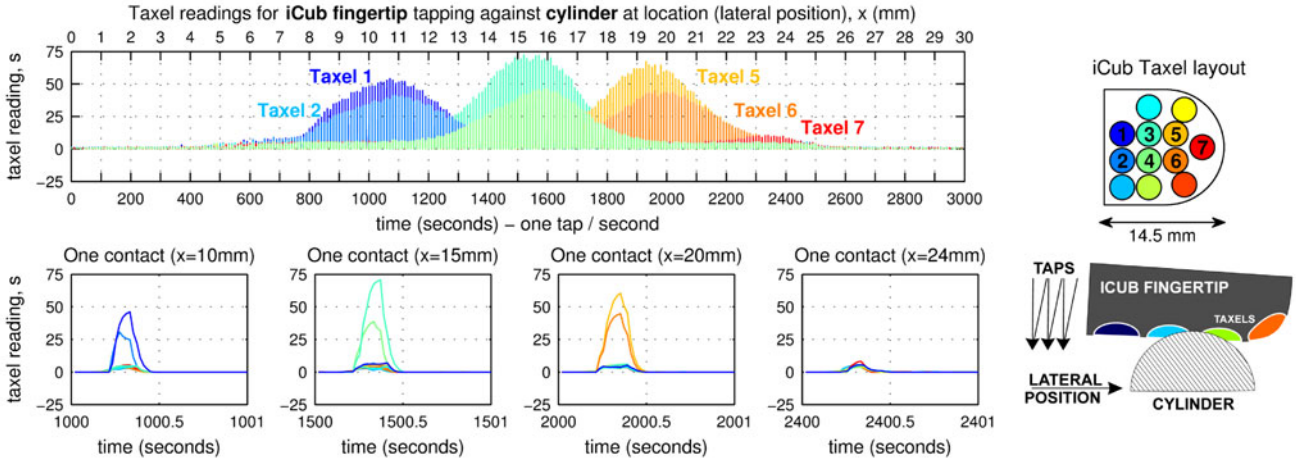

(b) Data for the capacitive tactile fingertip (iCub fingertip) tapping onto a cylinder (8 mm dia.) at location x (lateral position). Top: entire data set of 3000 taps over 30 mm range, plotted against time (each tap takes 1 sec). Bottom 4 panels: contact data from individual taps. The color of the plotted trace corresponds to the taxel locations (right figure) and the magnitude the taxel reading.

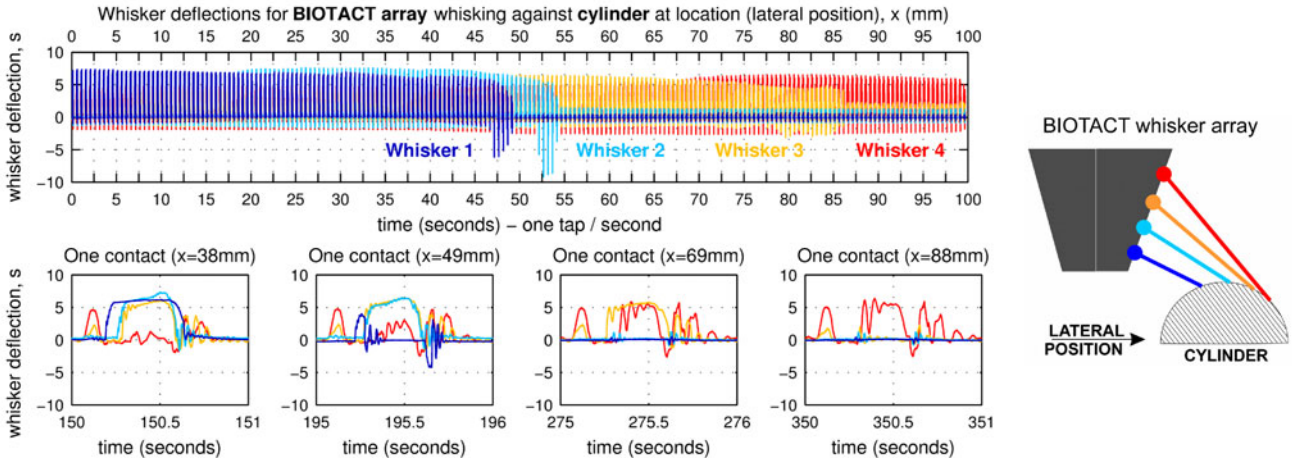

(c) Data for the whisker array (BIOTACT sensor) whisking against a cylinder (50 mm dia.) at location x (lateral position). Top: entire data set of 100 whisks over 100 mm range, plotted against time (each whisk takes 1 sec). Bottom 4 panels: contact data from individual whisks. The color of the plotted trace corresponds to the whisker (right figure) and the magnitude the whisker deflection at its base. Data collected in [46]; passive analysis in [29].

Fig. 6. Example data sets for the three tactile sensors (TacTip, iCub fingertip, and BIOTACT whisker array) considered in this study. All sets shown here are for cylindrical stimuli contacted with tapping/whisking motions over a range of lateral contact positions across their diameters. See Fig. 1 for the robots and experiment designs. This data is used to construct a virtual environment suitable for a Monte Carlo assessment (Section 5.1) of the relative performance of active and passive perception (Section 6).

considered here. All data were collected twice, to give independent training and testing data for use in validation.

For each sensor, the first experiment is essentially the same: cylinders contacted perpendicularly to their axes over a range of contact locations along the diameter of the cylinder. The TacTip and BIOTACT whisker array use a common collection of six cylinders (from 30 to 80 mm diameter), while due to its smaller size the iCub fingertip uses five smaller cylinders (from 4 to 12 mm). The BIOTACT whiskers are relatively fragile, permitting only 400 contacts per cylinder (over a 100 mm range) to ensure the whiskers did not need replacing mid-experiment; the iCub fingertip and TacTip are more robust, permitting 3,000 and 1,000 contacts each per cylinder (over 30 and 40 mm ranges). We used briefer taps (1 sec; 0.1 sec in contact) with the iCub fingertip because this sensor has greater hysteresis than the other sensors. The range of contact positions for the TacTip began and ended with tapping into mid-air; the iCub began with taps onto its rigid insensitive base and finished with taps into air. The span of positions was chosen based on the overall scale of the tactile sensor, to limit the number of non-contact data.

The second experiments are chosen to be different from both the first experiment and each other. For the TacTip, we consider 20 gaps of width 0.25-5 mm, with locations the contact depth in the direction perpendicular to the surface containing the gap (over a 5.5 mm range). For the iCub fingertip, we consider 12 grades of sandpaper (p60-p800), with contact depth over the surface also varying (over a 5.5 mm range). Finally, we consider a single non-actuated tactile whisker, with identity corresponding to the speed of contact (over a 36-216 mm/sec range) and location the contact distance radially along the whisker shaft (over a 30-80 mm range).

The choice of experiments was governed partly by availability of data from previous studies and partly by wanting to consider a wide variety of types of contact data. Both whisker experiments have been considered previously, but only using passive methods for perception [46], [47], [62]. One cylinder of the first data set for the TacTip and iCub fingertips has been considered before [6], [7], but the analysis was restricted to perception of contact location, not stimulus identity, in studies of tactile superresolution of location. The second experiments for the TacTip (gap width) and iCub fingertip (texture) have been examined before with active perception [29], [30]; however, those analyses differs from here in perspective and important technical details (e.g., optimizing the fixation point); moreover, the present study aims to give a synthetic view across many sensors and stimuli, rather than isolated examples.

The contact data for the two validation sets from each experiment is partitioned into N_{loc} discrete location and N_{id} distinct identity classes (details in Table 1). The location classes are uniform within each of the six experiments, in that each contains the same number of contacts and has the same span. Typically, the identity classes correspond to the distinct stimuli for each experiment (cylinder diameters, sandpaper type or gap width); for the second whisker experiment the identity is contact speed, which is partitioned into 20 classes of 9 mm/sec span each. The training data is used to learn the map from encoding contact data into increments of evidence (Section 4.3), and the test data as a virtual environment to draw data as if the sensor was perceiving from initially random (and unknown) locations and stimulus identities.

5.2 Monte Carlo Validation

Our experimental validation procedure assesses the methods for biomimetic perception off-line on data that realistically represents the real-time operation of the tactile sensor, permitting direct comparison of different algorithms with the same data. Automated data collection procedures are needed to collect large data sets that capture a 'virtual environment' that can be sampled from as if operating in real-time in a true environment. This motivates our use of robot arms and a Cartesian robot with high accuracy and repeatability for controlling the tactile sensor location (Section 3).

For robust validation of sensor and algorithm performance, a Monte carlo procedures is used with a standard testing/training validation methodology (10,000 iterations per data point). One dataset is used to train the biomimetic perception methods; then a distinct test set used to randomly and repeatedly generate runs over the range of initial contact locations with the various stimuli.

Our main performance measure is the identity 'what' error, given by the mean absolute error between the true identity class w and that perceived w_{dec} at a true location class x, and the mean decision times to reach that error

$$e_{\text{id}}(x,w) = \langle |w_{\text{dec}} - w| \rangle, \quad t_{\text{dec}}(x,w) = \langle t_{\text{dec}} \rangle \tag{21}$$

with the ensemble average $\langle \cdot \rangle$ evaluated over all test runs with the same true (x,w) classes. These identity errors and decision times are then averaged over both stimulus location and identity (x,w) to give an overall measure of performance

$$\bar{e}_{\text{id}} = \sum_{l=1}^{N_{\text{loc}}} \sum_{i=1}^{N_{\text{id}}} \frac{e_{\text{id}}(x_l, w_i)}{N_{\text{id}} N_{\text{loc}}}, \quad \bar{t}_{\text{dec}} = \sum_{l=1}^{N_{\text{loc}}} \sum_{i=1}^{N_{\text{id}}} \frac{t_{\text{dec}}(x_l, w_i)}{N_{\text{id}} N_{\text{loc}}}. \tag{22}$$

Note that these errors will depend on the control policy, such as the fixation point of active (focal) perception.

6 Results of Active and Passive Perception

Our main analysis is a comparison of active and passive biomimetic perception for perceiving the identities of a variety of test stimuli with the three distinct types of tactile sensor (TacTip, iCub fingertip, BIOTACT whisker). Biomimetic active perception has a control policy that re-locates the sensor based on evidence during the decision making process, here to a fixation point x_{fix} representing the focus of attention (Section 4.2.1); the location of this fixation point is described in a later analysis (Section 7; values shown on Fig. 8). This performance is compared to a passive stationary policy that cannot change percept class during the decision process (Section 4.2.2) and a passive random policy that randomly samples location classes (Section 4.2.3). Comparison between the active, stationary and random passive perception uses the test data as a virtual environment to randomly generate test runs, with a Monte Carlo analysis giving the mean errors and decision times (Section 5).

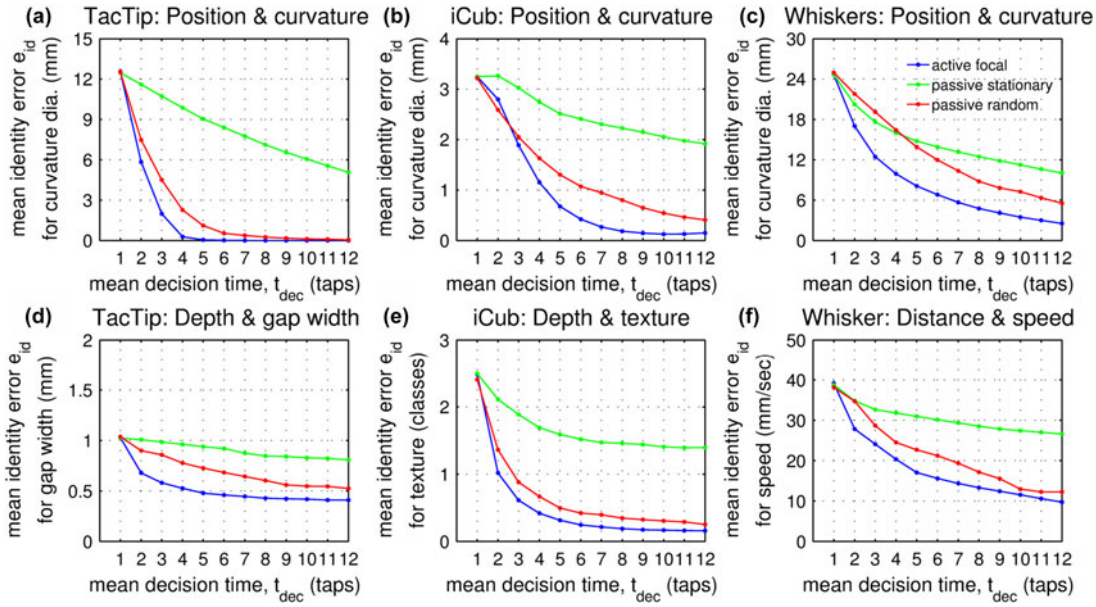

Fig. 7. Overall identification accuracy $\bar{e}_{\mathrm{id}}$ with mean decision time $\bar{t}_{\mathrm{dec}}$ for active focal (blue), passive stationary (green), and passive random (red) perception, averaged over both location and stimulus identity. Both the error and decision times are determined by the evidence threshold E_{dec}, which acts as an implicit parameter specifying the point along the speed-accuracy curves. Ten Thousand Monte Carlo iterations were used at each threshold, with random starting locations and stimulus identities, and the results interpolated to integer decision times. The results show that active perception is superior (lower error with decision time) to both forms of passive perception in all six experiments.

For active and both types of passive perception, variations of the decision errors $\bar{e}_{\mathrm{id}}$ with mean decision times $\bar{t}_{\mathrm{dec}}$ resemble the classic speed-accuracy tradeoff curves (Fig. 7) that are ubiquitous in human and animal psychology. Such tradeoffs follow from standard decision theory, since accuracy improves as more evidence is used to form a decision. Note that standard decision theory would have the asymptote at zero; here there is an important difference that the mean error can asymptote to nonzero values at long decision times (which occurs because the likelihood distributions from the training do not necessarily match those from testing).

Biomimetic active perception clearly gives superior performance to both stationary and random passive perception (Fig. 7) for decision times $t_{\mathrm{dec}} > 1$. In all cases, the error curves for active perception then lie below those of passive perception compared at the same decision time. (For $t_{\mathrm{dec}} = 1$ the sensor is unable to move so active and passive perception coincide.) Meanwhile, passive perception with a random control policy has better performance than a stationary policy, which we attribute to random perception sometimes sampling from a good location class even if it begins at poor location, unlike a stationary policy.

The tradeoff between errors and decision times is tuned by the evidence threshold E_{dec}, which acts as an implicit parameter specifying the point along the speed-accuracy curve. At the lowest thresholds, decisions require just one contact $t_{\mathrm{dec}} = 1$ and errors are most inaccurate. Identity errors $\bar{e}_{\mathrm{id}}$ then range from 13 mm (~25 percent) of a 50 mm range (TacTip, curvature) to 25 mm (~40 percent) of a 50 mm range (whisker, curvature). Increasing the evidence threshold results in slower and more accurate decisions. The best identity errors for active perception then range from 0 mm (0 percent) of a 50 mm range (TacTip, curvature) to 10 mm/s (~6 percent) of a 180 mm/s range (whisker, speed) over 12 taps (see Table 2).

Overall, for all sensors and all experiments, active perception based on focal attention reaches close to its best accuracy after 5-10 taps, with stimulus identification performance (0-6 percent) two orders of magnitude better than the sensor size and typically an order of magnitude better than the spacing between tactile elements (pins, taxels and whiskers).

TABLE 2
Best Accuracies (Minimal Errors $\bar{e}_{\mathrm{id}}$) for Active and Passive Perception Over 12 Contact Taps/Whisks

Sensor	active (focal) perception minimal error: $\bar{e}_{\mathrm{id}}$ (classes, range)	passive (random) perception minimal error: $\bar{e}_{\mathrm{id}}$ (classes, range)	passive (stationary) perception minimal error: $\bar{e}_{\mathrm{id}}$ (classes, range)
TacTip	0 mm curvature (0 classes; 0% range)	0 mm curvature (0 classes; 0% range)	5 mm curvature (0.5 classes; 10% range)
	0.3 mm gap width (1.2 classes; 6% range)	0.5 mm gap width (2 classes; 6% range)	0.8 mm gap width (2.6 classes; 6% range)
iCub fingertip	0.2 mm curvature (0.1 classes; 2% range)	0.4 mm curvature (0.2 classes; 4% range)	1.9 mm curvature (0.95 classes; 19% range)
	0.2 texture grades (0.2 classes; 2% range)	0.3 texture grades (0.3 classes; 3% range)	1.4 texture grades (1.4 classes; 14% range)
BIOTACT whisker	2 mm curvature (0.2 classes; 4% range)	6 mm curvature (0.6 classes; 12% range)	10 mm curvature (1.0 classes; 20% range)
	10 mm/sec speed (1 class; 6% range)	12 mm/sec speed (1.2 classes; 7% range)	27 mm/sec speed (2.7 classes; 16% range)

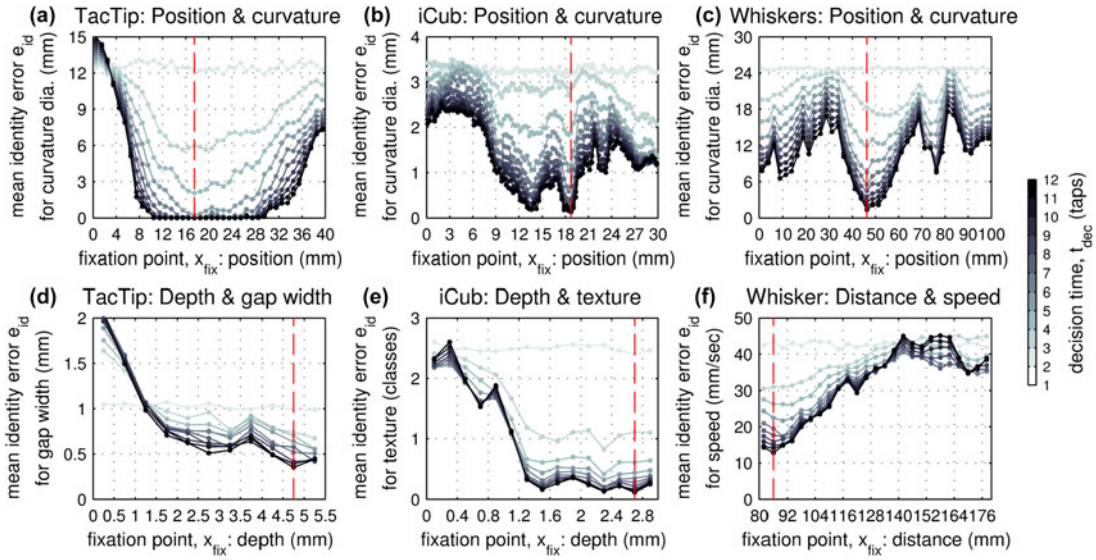

Fig. 8. Accuracy of biomimetic active perception with fixed point x_{fix} of focal attention, assessed with the mean identity error $\bar{e}_{\text{id}}(x)$ over all test stimuli and sensing locations (gray shading marks decision time). Evidently, sensing accuracy is highly dependent on the active control policy, with there being a well-defined global minimum for each experiment (red dashed line). This optimal fixed point is used for the active perception in Fig. 7.

7 Results of Optimizing Active Perception

Our next analysis examines the dependence of biomimetic active perception upon the fixation point x_{fix}, which is a free parameter specifying the focal attention of the active control policy. This analysis also serves to optimize the performance of active perception for each of the six experiments, the results of which were used in the previous section (Section 6). Perceptual performance is evaluated using the test data as a virtual environment to randomly generate test runs over the range of stimulus identities and locations, with a Monte Carlo analysis giving the mean errors and decision times similarly to the analysis in Section 6.

For all experiments, the decision errors $\bar{e}_{\text{id}}$ vary strongly with fixation point x_{fix} over the full location range (Fig. 8; shading denotes decision time $\bar{t}_{\text{dec}}$). The optimal location for fixation is shown the plots (red dashed line), corresponding to the location class with lowest error after 10 taps; these values were used as the fixation point x_{fix} in the previous section (Section 6 and Fig. 7).

The cylinder experiments for the three types of sensor (Figs. 8a, 8b, 8c) share a common result that the central region of the location range is best for fixation and the periphery worst. It appears that central contacts over the cylinders give better tactile information than glancing off-center contacts, as is expected. The local minima for the iCub fingertip (Fig. 8b) and whiskers (Fig. 8c) indicate further subtlety relating to how information is spread over the sensory receptors; for example, a slightly off-center contact on the cylinder appears optimal for the iCub fingertip.

The other three experiments (Figs. 8d, 8e, 8f) share a commonality that one extreme of location range is best for fixation and the other extreme the poorest. For the two tactile fingertips, the experiments are over contact depth (Figs. 8d, 8e), consistent with the poorer locations being those depths where the fingertips contact only weakly or not at all. For the tactile whisker, the experiment is over contact distance along the whisker shaft (Fig. 8f), consistent with the poorer locations corresponding to weaker (angular) displacements of the whisker caused by a contact near the tip.).

8 Discussion

Overall, biomimetic active touch accurately perceives the identity of many distinct types of stimuli (curved surfaces, textured surfaces, gaps in objects and radial contact distance) with three distinct biomimetic designs of tactile sensor: two biomimetic fingertips, the TacTip [5] optical tactile sensor and the iCub (capacitive) fingertip [4]; and a biomimetic whisker array [8], [9] based on the rodent vibrissal system. Movements during the active perception are considered over a variety of degrees of freedom (horizontal position, depth over the texture, depth over the gap, and speed of contact, respectively). Generally, the accuracy is well within a single stimulus identity class, with performance typically a couple of orders of magnitude better than the sensor size.

In general for all sensors and experiments, biomimetic touch with active control based on focal attention outperforms passive perception with static or random action selection. This performance originates from a strong dependence of tactile perception on object location relative to the sensor. Active perception assesses this relative location during the decision process to move the sensor to the best region for perception at the fixation point of focal attention, progressively improving the perceptual acuity.

8.1 Relation to Biological Perception

Biomimetic tactile perception is here based on three aspects of biological perception: sensory encoding of the stimulus as evidence, perceptual decision formation based on accumulating that evidence to threshold, and active selection of actions during the perceptual decision process. All three principles relate to important themes of ongoing research within neuroscience. Sensory encoding relates to the research area of neural coding that examines how information in the brain is represented by the pattern of activity across millions or

billions of interconnected neurons [63]. Perceptual decision formation as evidence accumulation to threshold is well established within psychology [64], but has recently received new life by the recognition that traditional methods are closely related to statistically optimal methods for decision formation [53]. The selection of actions during perception is closely related to research on overt attention, specifically focal attention [65], and more broadly towards a theory of consciousness based on the contingencies between sensing and acting [66].

That being said, even though our methods for perception are based on biomimetic principles there are also non-biomimetic aspects. For example, fingertip contacts are via taps, which are arguably not common as an exploratory procedure in humans [14]. That being said, we do use taps in some circumstances (e.g., palpation for medical diagnosis and when feeling sharp or hot objects); also tapping with fingertips is akin to whisking with vibrissae, which is the dominant exploratory procedure in rodents. Furthermore, the methods apply more generally to other modes of contacting surfaces, such as contour following akin to human tactile shape exploration [33].

In general, engineered biomimetic systems will always have some non-biomimetic aspects. This fits entirely within the spirit of biomimetics, which is to extract *principles* from biological systems that usefully apply to engineered systems [1], rather than faithfully copying all details of the natural system.

8.2 Superresolution and Hyperacuity

Active touch with focal attention perceived spatial location and spatial features to a fraction of a millimeter for the two fingertips and a couple of millimeters for the whiskers, an order of magnitude better than the spatial separation between the tactile elements comprising these sensors ($\sim$4 mm between pins/taxels for the tactile fingertips; 25 mm between whiskers). This effect, where spatial localization transcends the resolution of the sensor, is known as superresolution (engineering/optics) and hyperacuity (biology/physiology) [67], and has recently been demonstrated in related studies of biomimetic tactile fingertips [6], [7].

The biomimetic design of these tactile sensors is instrumental for this superresolution/hyperacuity. All three tactile sensors are based on collections of discrete sensing elements (pins, taxels and whiskers) each with receptive fields (areas sensitive to contact) broader than the spacing between elements, with contact sensitivity that varies smoothly within each field (Fig. 6). This structure of multiple, overlapping sensory receptive fields is fundamental to biological tactile sensing also, and underlies an organizational principle whereby multiple neurons represent a single stimulus in a distributed manner. In consequence of the stimulus representation being distributed, statistical interpolation over spatial features can result in an accuracy that transcends the sensor resolution set by the spacing between adjacent sensory receptors.

8.3 Active and Passive Biomimetic Perception

Biomimetic perception combines decision formation with a control policy for moving the sensor (Fig. 4) based on sensory evidence. This policy implements action selection to help perceive or explore a stimulus [14]. Active perception has a closed-loop control policy [2] that depends on the accumulated evidence during the decision process; passive perception has an open-loop policy independent of evidence.

Biomimetic active perception was considered with evidence-based action selection based on focal attention, implemented as a control policy that makes a best move to a fixation point based on evidence for the present location. This control policy enables robust perception of stimulus identity ('what') when the sensing is strongly location ('where') dependent. For the experiments considered here, this fixed point was typically at an obvious location, such as the center of an object or at a sufficiently strong contact depth. Fine tuning was also necessary to achieve the best perception (for example, the iCub fingertip; Fig. 8b). These results are compatible with previous assessments of a related method of active Bayesian perception with the iCub fingertip [10], [29].

In comparison, biomimetic passive perception was considered with random and stationary [56], [62] control policies that make random or no movements. Of the two passive policies, the random action selection gave better performance because it partially overcame the strong location dependence of perception by sampling the entire range. However, the random policy did require far more movement and still had poorer performance than active perception with focal attention.

Other action selection policies could be appropriate in different scenarios. For example, an approach of Bayesian exploration considered an active control policy that moves a biomimetic fingertip (to control force and speed) to best disambiguate the identification of many textures [25], [26]. Another study considered a control policy for contour following to explore an object's shape [33].

9 Conclusions

Biomimetic active perception offers a general approach for robot touch with biomimetic sensors ranging from tactile fingertips to whiskers. Biomimetic tactile sensors are commonly based on analogous receptive field structures to their biological counterparts. By using principles of animal perception, biomimetic perception seeks to make best use of these properties of biomimetic sensors: neuronal population encoding of stimuli as evidence; perceptual decision formation by evidence accumulation; and focal attention as action selection during perception. These principles of biomimetic active perception enable robust and accurate perception in situations of uncertain stimulus location ('where') and identity ('what'), as faced by animals and robots in natural, complex environments.

Acknowledgments

The author would like to thank his colleagues who contributed to this theme of work: Tony Prescott, Uriel Martinez-Hernandez, Ben Ward-Cherrier, Mat Evans, Ben Mitchinson, Charles Fox, Martin Pearson, Charlie Sullivan, and Giorgio Metta. This work was supported by a grant from the Engineering and Physical Sciences Research Council (EPSRC) on "Tactile Superresolution Sensing" (EP/M02993X/1). The data used in this letter can be accessed at http://lepora.com/publications/lepora2016toh_data

REFERENCES

[1] N. Lepora, P. Verschure, and T. Prescott, "The state of the art in biomimetics," *Bioinspiration Biomimetics*, vol. 8, no. 1, 2013, Art. no. 013001.

[2] R. Bajcsy, "Active perception," *Proc. IEEE*, vol. 76, no. 8, pp. 966–1005, Aug. 1988.

[3] J. Gibson, *The Senses Considered as Perceptual Systems*. Houston, TX, USA: Houghton Mifflin, 1966.

[4] A. Schmitz, P. Maiolino, M. Maggiali, L. Natale, G. Cannata, and G. Metta, "Methods and technologies for the implementation of large-scale robot tactile sensors," *IEEE Trans. Robot.*, vol. 27, no. 3, pp. 389–400, May 2011.

[5] C. Chorley, C. Melhuish, T. Pipe, and J. Rossiter, "Development of a tactile sensor based on biologically inspired edge encoding," in *Proc. Int. Conf. Adv. Robot.*, 2009, pp. 1–6.

[6] N. F. Lepora, U. Martinez-Hernandez, M. Evans, L. Natale, G. Metta, and T. J. Prescott, "Tactile superresolution and biomimetic hyperacuity," *IEEE Trans. Robot.*, vol. 31, no. 3, pp. 605–618, Apr. 2015.

[7] N. Lepora and B. Ward-Cherrier, "Superresolution with an optical tactile sensor," in *Proc. IEEE/RSJ Int. Conf. Intell. Robots Syst.*,2015, pp. 2686–2691.

[8] J. Sullivan, et al., "Tactile Discrimination using Active Whisker Sensors," *IEEE Sensors*, vol. 12, no. 2, pp. 350–362, Apr. 2012.

[9] M. Pearson, B. Mitchinson, J. Sullivan, A. Pipe, and T. Prescott, "Biomimetic vibrissal sensing for robots," *Philosoph. Trans. Roy. Soc. London B, Biol. Sci.*, vol. 366, no. 1581, pp. 3085–3096, 2011.

[10] N. Lepora, U. Martinez-Hernandez, and T. Prescott, "Active Bayesian perception for simultaneous object localization and identification," in *Robotics: Science and Systems*. Cambridge, MA, USA: MIT Press, 2013.

[11] T. Prescott, M. Diamond, and A. Wing, "Active touch sensing," *Philosoph. Trans. Roy. Soc. B, Biol. Sci.*, vol. 366, no. 1581, pp. 2989–2995, 2011.

[12] N. Lepora, "Active tactile perception," in *Scholarpedia of Touch*. Amsterdam, Netherlands: Atlantis Press,2016, pp. 151–159.

[13] J. Gibson, "Observations on active touch," *Psychological Rev.*, vol. 69, no. 6, pp. 477–491, 1962.

[14] S. Lederman and R. Klatzky, "Hand movements: A window into haptic object recognition," *Cogn. Psychol.*, vol. 19, pp. 342–368, 1987.

[15] S. Stansfield, "Primitives, features, and exploratory procedures: Building a robot tactile perception system," in *Proc. IEEE Int. Conf. Robot. Autom.*,1986, vol. 3, pp. 1274–1279.

[16] R. Bajcsy, S. J. Lederman, and R. L. Klatzky, "Object exploration in one and two fingered robots," in *Proc. IEEE Int. Conf. Robot. Autom.*,1987, vol. 3, pp. 1806–1810.

[17] H. Maekawa, K. Tanie, K. Komoriya, M. Kaneko, C. Horiguchi, and T. Sugawara, "Development of a finger-shaped tactile sensor and its evaluation by active touch," in *Proc. IEEE Int. Conf. Robot. Autom.*,1992, pp. 1327–1334.

[18] M. Shimojo and M. Ishikawa, "An active touch sensing method using a spatial filtering tactile sensor," in *Proc. IEEE Int. Conf. Robot. Autom.*,1993, pp. 948–954.

[19] A. Okamura and M. Cutkosky, "Feature detection for haptic exploration with robotic fingers," *Int. J. Robot. Res.*, vol. 20, no. 12, pp. 925–938, 2001.

[20] M. Kaneko and K. Tanie, "Contact point detection for grasping an unknown object using self-posture changeability," in *Proc. IEEE Int. Conf. Robot. Autom.*,1994, vol. 10, no. 3, pp. 355–367.

[21] M. Cutkosky, R. Howe, and W. Provancher, "Force and tactile sensors," in *Springer Handbook of Robotics*. Berlin, Germany: Springer-Verlag,2008, pp. 455–476.

[22] C. Oddo, M. Controzzi, L. Beccai, C. Cipriani, and M. Carrozza, "Roughness encoding for discrimination of surfaces in artificial active-touch," *IEEE Trans. Robot.*, vol. 27, no. 3, pp. 522–533, Apr. 2011.

[23] L. Pape, C. Oddo, M. Controzzi, C. Cipriani, A. Förster, M. Carrozza, and J. Schmidhuber, "Learning tactile skills through curious exploration," *Frontiers Neurorobotics*, vol. 6, pp. 35–50, 2012.

[24] Z. Su, J. A. Fishel, T. Yamamoto, and G. E. Loeb, "Use of tactile feedback to control exploratory movements to characterize object compliance," *Frontiers Neurorobotics*, vol. 6, 2012.

[25] J. Fishel and G. Loeb, "Bayesian exploration for intelligent identification of textures," *Frontiers Neurorobotics*, vol. 6, 2012.

[26] G. Loeb and J. Fishel, "Bayesian action & perception: Representing the world in the brain," *Frontiers Neurosci.*, vol. 8, 2014.

[27] V. Chu, I. McMahon, L. Riano, C. G. McDonald, Q. He, J. M. Perez-Tejada, M. Arrigo, T. Darrell, and K. J. Kuchenbecker, "Robotic learning of haptic adjectives through physical interaction," *Robot. Auton. Syst.*, vol. 63, pp. 279–292, 2015.

[28] R. Martins, J. Ferreira, and J. Dias, "Touch attention Bayesian models for robotic active haptic exploration of heterogeneous surfaces," in *Proc. IEEE/RSJ Int. Conf. Intell. Robots Syst.*,2014, pp. 1208–1215.

[29] N. Lepora, U. Martinez-Hernandez, and T. Prescott, "Active touch for robust perception under position uncertainty," in *Proc. IEEE Int. Conf. Robot. Autom.*,2013, pp. 3005–3010.

[30] N. Lepora and B. Ward-Cherrier, "Tactile quality control with biomimetic active touch," *IEEE Robot. Autom. Lett.*, vol. 1, no. 2, pp. 646–652, Jul. 2016.

[31] B. Ward-Cherrier, L. Cramphorn, and N. Lepora, "Tactile manipulation with a TacThumb integrated on the open-hand M2 gripper," *IEEE Robot. Autom Lett.*, vol. 1, no. 1, pp. 169–175, Jan. 2016.

[32] L. Cramphorn, B. Ward-Cherrier, and N. Lepora, "Tactile manipulation with biomimetic active touch," in *Proc. IEEE Int. Conf. Robot. Autom.*, 2016, pp. 123–129.

[33] U. Martinez-Hernandez, T. Dodd, L. Natale, G. Metta, T. Prescott, and N. Lepora, "Active contour following to explore object shape with robot touch," in *Proc. World Haptics Conf.*,2013, pp. 341–346.

[34] M. Kaneko, N. Kanayama, and T. Tsuji, "Active antenna for contact sensing," *IEEE Trans. Robot. Autom.*, vol. 14, no. 2, pp. 278–291, Apr. 1998.

[35] M. Fend, S. Bovet, H. Yokoi, and R. Pfeifer, "An active artificial whisker array for texture discrimination," in *Proc. IEEE/RSJ Int. Conf. Intell. Robots Syst.*,2003, vol. 2, pp. 1044–1049.

[36] M. Pearson, A. Pipe, C. Melhuish, B. Mitchinson, and T. Prescott, "Whiskerbot: A robotic active touch system modeled on the rat whisker sensory system," *Adapt. Behav.*, vol. 15, no. 3, pp. 223–240, 2007.

[37] T. Prescott, M. Pearson, B. Mitchinson, J. Sullivan, and A. Pipe, "Whisking with robots from rat vibrissae to biomimetic technology for active touch," *IEEE Robot. Autom. Mag.*, vol. 16, no. 3, pp. 42–50, Sep. 2009.

[38] C. Fox, B. Mitchinson, M. Pearson, A. Pipe, and T. Prescott, "Contact type dependency of texture classification in a whiskered mobile robot," *Auton. Robot.*, vol. 26, no. 4, pp. 223–239, 2009.

[39] B. Winstone, G. Griffiths, T. Pipe, C. Melhuish, and J. Rossiter, "TACTIP-tactile fingertip device, texture analysis through optical tracking of skin features," in *Biomimetic and Biohybrid Systems*. Berlin, Germany: Springer-Verlag,2013, pp. 323–334.

[40] T. Assaf, C. Roke, J. Rossiter, T. Pipe, and C. Melhuish, "Seeing by touch: Evaluation of a soft biologically-inspired artificial fingertip in real-time active touch," *Sensors*, vol. 14, no. 2, pp. 2561–2577, 2014.

[41] U. Martinez-Hernandez, "Tactile sensors," *Scholarpedia*, vol. 10, no. 4,2015, Art. no. 32398.

[42] Y. Lee and K. Wise, "A batch-fabricated silicon capacitive pressure transducer with low temperature sensitivity," *IEEE Trans. Electron Devices*, vol. 29, no. 1, pp. 42–48, Jan. 1982.

[43] G. Metta, G. Sandini, D. Vernon, L. Natale, and F. Nori, "The ICUB humanoid robot: an open platform for research in embodied cognition," in *Proc. 8th Workshop Intell. Syst.*,2008, pp. 50–56.

[44] P. Schmidt, E. Maël, and R. Würtz, "A sensor for dynamic tactile information with applications in human-robot interaction and object exploration (is this right?)" *Robot. Auton. Syst.*, vol. 54, no. 12, pp. 1005–1014, 2006.

[45] H. Muhammad, C. Oddo, L. Beccai, C. Recchiuto, C. Anthony, M. Adams, M. Carrozza, D. Hukins, and M. Ward, "Development of a bioinspired MEMS based capacitive tactile sensor for a robotic finger," *Sensors Actuators A, Phys.*, vol. 165, no. 2, pp. 221–229, 2011.

[46] M. Evans, C. Fox, M. Pearson, N. Lepora, and T. Prescott, "Whisker-object contact speed affects radial distance estimation," in *Proc. IEEE Int. Conf. Robot. Biomimetics*,2010, pp. 720–725.

[47] M. Evans, C. Fox, N. Lepora, M. Pearson, J. Sullivan, and T. Prescott, "The effect of whisker movement on radial distance estimation: A case study in comparative robotics," *Frontiers Neurorobotics*, vol. 6, 2012.

[48] N. Lepora, U. Martinez-Hernandez, H. Barron-Gonzalez, M. Evans, G. Metta, and T. Prescott, "Embodied hyperacuity from Bayesian perception: Shape and position discrimination with an ICUB fingertip sensor," in *Proc. IEEE/RSJ Int. Conf. Intell. Robots Syst.*,2012, pp. 4638–4643.

[49] N. Lepora, U. Martinez-Hernandez, G. Pezzulo, and T. Prescott, "Active Bayesian perception and reinforcement learning," in *Proc. IEEE/RSJ Int. Conf. Intell. Robots Syst.*,2013, pp. 4735–4740.
[50] A. Pipe and M. Pearson, "Whiskered robots," *Scholarpedia*, vol. 10, no. 3,2015, Art. no. 6641.
[51] B. Mitchinson, T. Chan, J. Chambers, M. Pearson, M. Humphries, C. Fox, K. Gurney, and T. Prescott, "Brahms: Novel middleware for integrated systems computation," *Adv. Eng. Inf.*, vol. 24, no. 1, pp. 49–61, 2010.
[52] T. Perkins and P. Swain, "Strategies for cellular decision-making," *Molecular Syst. Biol.*, vol. 5, no. 1,2009, Art. no. 326.
[53] R. Bogacz, E. Brown, J. Moehlis, P. Holmes, and J. Cohen, "The physics of optimal decision making: A formal analysis of models of performance in two-alternative forced-choice tasks," *Psychological Rev.*, vol. 113, no. 4, pp. 700–765, 2006.
[54] D. Sumpter, "The principles of collective animal behaviour," *Philosoph. Trans. Roy. Soc. B, Biol. Sci.*, vol. 361, no. 1465, pp. 5–22, 2006.
[55] A. Wald and J. Wolfowitz, "Optimum character of the sequential probability ratio test," *Ann. Math. Stat.*, vol. 19, no. 3, pp. 326–339, 1948.
[56] N. Lepora, C. Fox, M. Evans, M. Diamond, K. Gurney, and T. Prescott, "Optimal decision-making in mammals: Insights from a robot study of rodent texture discrimination," *J. Roy. Soc. Interface*, vol. 9, no. 72, pp. 1517–1528, 2012.
[57] N. Lepora and K. Gurney, "The basal ganglia optimize decision making over general perceptual hypotheses," *Neural Comput.*, no. 24, pp. 2924–2945, 2012.
[58] T. Prescott, "Action selection," *Scholarpedia*, vol. 3, no. 2,2008, Art. no. 2705.
[59] T. Prescott, J. Bryson, and A. Seth, "Introduction. Modelling natural action selection," *Philosoph. Trans. Roy. Soc. London B, Biol. Sci.*, vol. 362, no. 1485, pp. 1521–1529, 2007.
[60] J. Wooldridge, *Introductory Econometrics: A Modern Approach*. Boston, MA, USA: Cengage Learning, 2009.
[61] N. Lepora, M. Evans, C. Fox, M. Diamond, K. Gurney, and T. Prescott, "Naive Bayes texture classification applied to whisker data from a moving robot," in *Proc. Int. Joint Conf. Neural Networks*,2010, pp. 1–8.
[62] N. Lepora, J. Sullivan, B. Mitchinson, M. Pearson, K. Gurney, and T. Prescott, "Brain-inspired Bayesian perception for biomimetic robot touch," in *Proc. IEEE Int. Conf. Robot. Autom.*,2012, pp. 5111–5116.
[63] A. Borst and F. Theunissen, "Information theory and neural coding," *Nature Neurosci.*, vol. 2, no. 11, pp. 947–957, 1999.
[64] R. Ratcliff, "A theory of memory retrieval," *Psychological Rev.*, vol. 85, no. 2,1978, Art. no. 59.
[65] L. Itti and C. Koch, "Computational modelling of visual attention," *Nature Rev. Neurosci.*, vol. 2, no. 3, pp. 194–203, 2001.
[66] J. K. O'Regan and A. Noë, "A sensorimotor account of vision and visual consciousness," *Behav. Brain Sci.*, vol. 24, no. 05, pp. 939–973, 2001.
[67] G. Westheimer, "Visual acuity and hyperacuity," *Handbook of Optics, Vol. III: Vision and Vision Optics*. New York, NY, USA: McGraw-Hill, 2009, pp. 4–1.

Nathan F. Lepora received the BA degree in mathematics from the University of Cambridge, United Kingdom, the MSc degree in robotics from the Department of Engineering Mathematics, University of Bristol (UOB), United Kingdom, and the PhD degree in theoretical physics from the University of Cambridge, United Kingdom. He is a lecturer and program director with the Department of Engineering Mathematics, UOB, United Kingdom. He is also with the Bristol Robotics Laboratory, UOB and UWE, United Kingdom. His research interests include robot and animal perception, artificial and natural decision making, and biomimetics. He is a member of the IEEE.

▷ **For more information on this or any other computing topic, please visit our Digital Library at** www.computer.org/publications/dlib.